P-103: Novel Poly-Si TFT Pixel Electrode Circuits and Current Programmed Active-Matrix Driving Methods for AM-OLEDs

Yongtaek Hong and Jerzy Kanicki
Solid-State Electronics Lab., Dept. of EECS, The University of Michigan, Ann Arbor, MI, USA
Reiji Hattori
Dept. of Electronic Device Eng., Kyushu University, Higashi-ku, Fukuoka, Japan

Abstract

In this paper, we present the systematic analysis of the current-programmed poly-Si pixel electrode circuits with current-sink-type charging functionality and duty ratio controllability. Two different driving schemes for top-cathode and top-anode organic light-emitting device structures are described and compared. Their limitations and advantages are also discussed.

1. Introduction

As organic and polymeric light-emitting device (OLED) technology mature, tremendous attentions have been paid to their implementation into the flat panel displays (FPDs). Several groups have focused their research to develop passive 0 - (PM) and active- matrix (AM) [4][8][[9] driving schemes for the FPDs. In the case of the PM-OLED, the selecting time of each pixel decreases as the resolution of the displays increases, requiring higher peak OLED brightness, i.e. large currents and voltages for each pixel are needed to obtain appropriate average FPD brightness levels. The increase of the crosstalk among pixels with increasing FPD resolution is another limitation of the PM-OLED. Since Dawson *et al.* [1] reported the four-thin-film transistors (TFTs) based AM-driving scheme, considerable efforts have been exerted to implement AM-OLEDs. [4][8][9] Because the OLED brightness is directly related to the current flow through the device, it is critical to achieve a constant current flow through the OLED to control the FPD brightness uniformity, which can be affected by TFTs threshold voltage and OLEDs turn-on voltage variations. To compensate for these variations, in our laboratory, we have adopted current-programmed AM-driving schemes based on four hydrogenated amorphous silicon TFTs (a-Si:H TFTs) and one selection line. [4] In our initial approach, there were several limitations such as OLED data current saturation and storage capacitor location dependence. Then, later we proposed improved a-Si:H TFTs pixel electrode circuits with two selection lines [5]. Also by extending this technology to polysilicon TFTs AM-OLED, we have successfully integrated the current-programmed driving circuits, based on digital-to-analog-converter (DAC), with the pixel electrode circuits. [3] While current-mirror based pixel electrode circuits can cause brightness variation if there is any mismatch between current driving pairs, this effect can be reduced in our driving scheme since data current directly flows through the driving TFT during storage capacitor charging time. With two separated selection lines, we can also control the duty ratio of current signal through the OLEDs, resulting in a high quality fast moving image by changing the light emission holding time. However, the simulations of our pixel circuit indicated that there is a current peak signal during the select transient especially when the data line has been previously charged. [3] This current peak may damage the OLEDs and may set error current at low data current values. To overcome these limitations, in this paper, we propose a current-sink type novel pixel electrode circuit consisting of four p-type or n-type poly-Si TFTs to be used for top-cathode and top-anode OLED structures, respectively.

2. Simulation details

AIM-SPICE has been used in this study to simulate the pixel electrode circuits based on four polysilicon TFTs. The parameters for polysilicon TFTs have been extracted from measured I_D-V_{GS} and I_D-V_{DS} characteristics by using AIM-EXTRACT tools, which are summarized in Table 1. The dimensions of p-type and n-type polysilicon transistors are described in Table 2. Since the gate length of all the TFTs is equal to or larger than 10 μm, we expect that the short channel effects are not severe in our case. The storage and data-line-parasitic capacitor values, and DC supply voltage for each circuit configuration (Fig. 2 and Fig. 3) are also included. The parameters for OLED with top-cathode structure have been extracted by using AIM-SPICE LED model, which are described in Table 3. The simulation curves were fitted to the measured OLED results over turn-on regions, which are defined as the current/voltage regions producing brightness larger than 1 cd/m^2. However, since the measurement data for the OLED with top-anode structure are not available at this time in our laboratory, the extracted parameters from the top-cathode OLED characteristics were used for top-anode OLED in these simulations. The OLED area was defined from 300×100 μm^2 pixel size assuming 25% aperture ratio. Considering display with 200 cd/m^2 brightness, at least 200/25% cd/m^2 brightness is needed for each pixel, e.g., 800 cd/m^2 brightness is needed for 0.75×10^{-4} cm^2 OLED area. For our organic polymer red light-emitting devices [6], about 90 mA/cm^2 is needed for 800 cd/m^2 brightness; thus, about 7 μA per pixel is needed for 0.75×10^{-4} cm^2 OLED. However, if we change the duty ratio of OLED light emission, which are defined as the ratio of light-emission holding time to the total frame time, higher brightness will be needed, e.g., for 50% duty ratio, we need at least 1600 cd/m^2 of brightness, thus about 14 μA current will be flowing through 0.75×10^{-4} cm^2 device considering our red polymer OLED performances. Therefore, all the simulation component parameters and conditions were selected for the pixel electrode circuit to provide up to 20 μA with the linear relationship between I_{data} and I_{OLED}. The simulation results of I_{OLED} versus I_{data} for several V_{dd} values for four p-type polysilicon TFT pixel electrode circuit (Fig. 2(a)) are shown in Fig. 1. I_{OLED} was measured during the frame time after I_{data} charges up the storage capacitor during select time. (Fig. 2(b)) It is noted that if V_{dd} increases, the maximum I_{data} current sustaining the linear relationship will also increase. Similar characteristics between I_{OLED} versus I_{data} for several V_{dd} have also been obtained for four n-type polysilicon TFT pixel electrode circuit (Fig. 3(a)). For polysilicon TFTs [7] and OLED [1], the parameters extracted from other groups are also included in the tables for reference.

 ISSN/0002-0966X/02/3301-0618-$1.00+.00

Table 1. Parameters for AIM-SPICE polysilicon TFT model (Temperature effects are not included in our simulations).

	Our work		*Literature [7]*	
	(p-type)	*(n-type)*	*(p-type)*	*(n-type)*
asat	0.93	0.96	0.60	0.87
at	3e-8	1.3e-8	5e-8	3e-8
blk	0.001	0.001	0.001	0.001
bt	0	0	0	0
dd	1.4e-7	2.0e-7	1.4e-7	1.4e-7
delta	4	4	4	4
dg	2e-7	1.3e-7	2e-7	2e-7
eb	0.68	0.68	0.68	0.68
eta	3	6.6	15	7
io	6	6	60	6
ioo	150	150	150	150
lasat	0	0	1.1e-6	6.7e-7
lkink	1e-7	1.5e-5	6.5e-6	1.9e-5
mkink	1.3	1.1	1.2	1.3
mmu	3	3	3	3
mul	2.2e-3	1.7e-3	2.9e-4	2.2e-3
muo	70	89	57	100
mus	1	0.55	0.0011	0.32
rd	50	500	N/A	500
rs	50	500	N/A	500
tox	1e-7	1e-7	1e-7	1e-7
vfb	-0.1	-0.1	-0.1	-0.1
vkink	20	6.6	6.5	9.1
vto	-2	2	-1	0.9

Table 2. Dimensions of TFTs and storage/data-line-parasitic capacitor values used in SPICE simulation.

	Fig.1	*Fig.2*
L (μm)	10 (T1, T2, T4) 30 (T3)	10 (T1, T2, T4) 30 (T3)
W (μm)	10 (T1, T2, T4) 50 (T3)	10 (T1, T2, T4) 50 (T3)
Cs (F)	0.1e-12	0.1e-12
Cp (F)	10e-12	10e-12
V_{dd_supply} (V)	13	14

Table 3. OLED parameters used in SPICE simulation.

	Our Red OPLED	*Literature [1]*
is (A/cm^2)	9.6e-6	1e-7
rs (ohm)	0	80
n	46.4	30
cjo (F/cm^2)	25e-9[1]	25e-9
A (cm^2)	0.75e-4	N/A

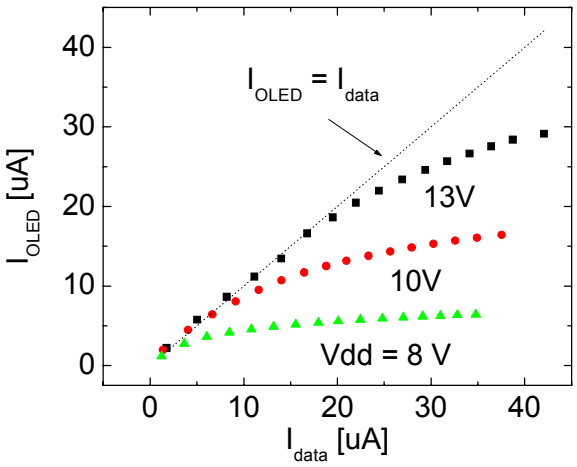

Figure 1. I_{OLED} versus I_{data} for several V_{dd} values simulated for four p-type poly-Si pixel electrode circuit (Fig. 2(a)) is shown. I_{OLED} was measured during the frame time after I_{data} charge up the storage capacitor during the select time (Fig. 2(b)). It is noted that I_{OLED} saturates as I_{data} increases and the maximum I_{data} sustaining the linear relationship increases as V_{dd} increases.

3. Simulation result and discussion

Figure 2 shows the pixel electrode circuit configuration based on four p-type poly-Si TFTs for top-cathode OLED structure AM-OLED and corresponding simulated waveforms, where the light will be emitted through the bottom electrode of the pixel. The T1/T2, T3, and T4 are selecting, switching, and driving TFTs, respectively. The T_1/T_2 and T_3 control the current flow path according to appropriate selecting voltage signals ($V_{select1}$ and $V_{select2}$). The period and select time of $V_{select1}$ and $V_{select2}$ waveforms have been selected as 16.7 ms and 34 μs considering 60Hz, VGA (640 × 480) display operation, respectively. During select time, T_1/T_2 are ON and T_4 is OFF, directing the data current flow from source line (V_{dd}) to data line through T_3 and T_2, which is indicated as a solid line in Fig. 2(a). After the C_S is charged up during select time, $V_{select1}$ and $V_{select2}$ signals change during frame time, turning T_1/T_2 OFF and T_4 ON, respectively. Then, the data current will flow from V_{dd} to ground through T_3, T_4, and OLED, which is indicated as a dotted line in Fig. 2(a). The high and low values of $V_{select1}$ and $V_{select2}$ are 13 and -3 V, and 11 and 3 V,

respectively. $V_{select2}$ waveform was selected to produce 80% of duty ratio for light emission, which will turn on T3 and supply current flow through the OLED over only 80% of the frame time. As mentioned before the duty ratio can be easily changed by changing $V_{select2}$ waveform. V_{OLED} and V_{Cs} are voltage drop across the OLED and storage capacitor, respectively. I_{data}, I_{OLED}, and I_{Vdd} are current flow at data line, through OLED, and from V_{dd},

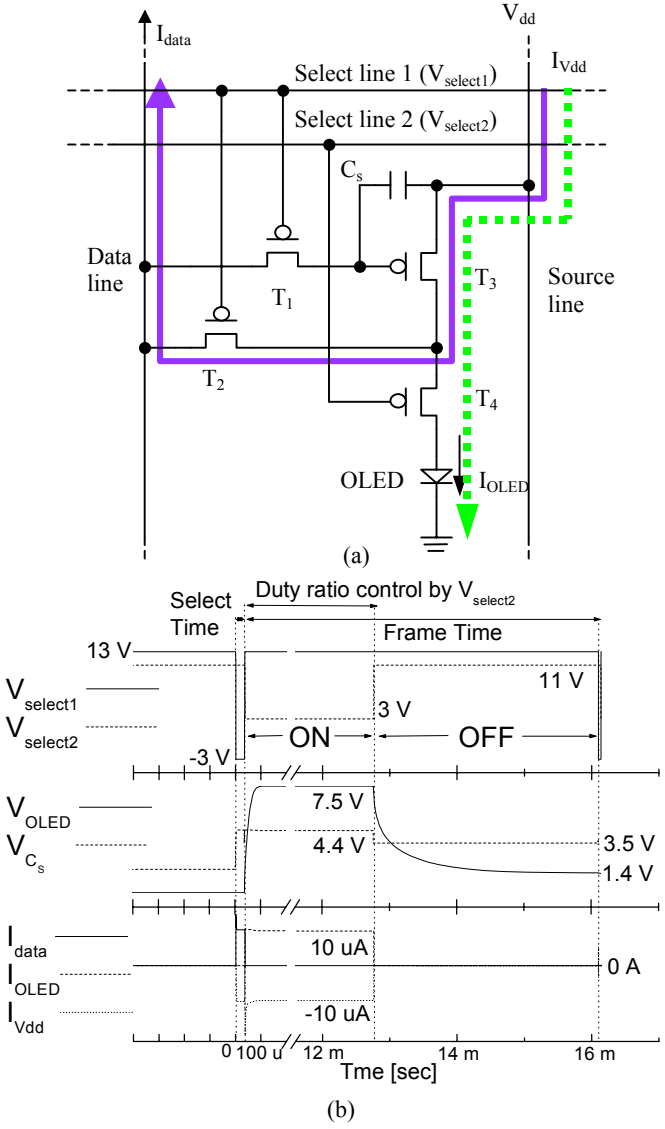

Figure 2. Four p-type poly-Si pixel electrode circuit for top-cathode OLED structure and signal waveforms are shown. The bold arrow shows the current flow path charging storage capacitor (C_s) during the select time. The simulation result shows that there is no current flow through the OLED ($I_D = 0$) during the select time to prevent the current transient peak from flowing through the device. It is noted that the duty ratio of the data current can also be controlled by changing $V_{select2}$ waveform for high quality fast moving images.

respectively, as indicated in Fig. 2(a). It is noted that the sign of each current (+ for I_{data} and I_{OLED}, - for I_{Vdd}) shows only the direction of the current flow. The I_{data} has the waveform with high value of 10 μA during 34 μs duration and low value of 0 A during the rest of 2×16.7 ms period. The storage capacitor is charged up to about 4.4 V during the select time and sustains this voltage during ON-time defined by the duty ratio. OLED starts to be charged up to about 7.5 V at the beginning of the frame time and it sustains this value during ON-time. Then, after $V_{select2}$ signal changes to high value, V_{Cs} abruptly decreases to 3.5 V and sustains this value, and V_{OLED} decreases to 1.4 V during the OFF-time, respectively. The V_{Cs} change is caused by abrupt cut-off of the current flow through the OLED, T_3, and T_4 during the $V_{select2}$ transition. The change of V_{Cs} is small during the ON- to OFF-period, and it is noted that $V_{select1}$ high value is carefully selected to avoid any significant leakage current through the T_1 and T_2 during OFF-time. The V_{OLED} initially decreases at a faster rate, and then at much slower rate during the OFF-time. This change of V_{OLED} variation can also be explained by the cut-off of the current flow. Since we speculate that the OLED is mainly discharging through the device itself, the change of V_{OLED} decrease rate can be explained by the OLED effective resistance change with applied bias. In this case, we assume that OLED can be simply modeled by a combination of a variable capacitor and a variable resistance. As indicated in Fig. 2(b) the data current starts to flow through the OLED after select time ends. The I_{OLED} current peak at the beginning of the frame time is suppressed by optimizing the $V_{select2}$ high and low values. This current peak can be caused by the abrupt change of the gate voltage of T_4 to the low value of $V_{select2}$ signal while the source voltage of T_4 is equal to T_3 gate voltage during the $V_{select1}$ and $V_{select2}$ transition. This abrupt voltage change can also cause T_3 to temporarily operate in the kink regime by increasing T_3 V_{DS}, thus the current peak can be observed during the voltage transition. Therefore, if a low value of $V_{select2}$ is not appropriately selected, the sudden change of T_4 gate voltage can cause the current peak during the voltage transition. However, the huge current peak during the voltage transition, which was observed for the circuit that the data line is directly coupled to OLED during the select time [3] is absent in this case. Since the data line is decoupled from OLED in this circuit, there is no current flow through the OLED during the select time. Also, as simulated above, this circuit has the duty ratio controllability of the OLED light emission by changing $V_{select2}$ waveform, which is important if we want to produce a high quality fast moving images. [9]

Similar pixel electrode circuit configuration and operation can also be suggested for AM-OLED with top-anode OLED structure as shown in Fig. 3, where the light will be emitted through the top-anode of the pixel. Like in the previous pixel circuit configuration, the T_1/T_2, T_3, and T_4 are selecting, switching, and driving TFTs, respectively. The T_1/T_2 and T_3 control the current flow path according to appropriate selecting voltage signals. During select time, T_1/T_2 are ON and T_4 is OFF, directing the data current flow from data line to the source line (GND) through T_2 and T_3, which is indicated as a solid line in Fig. 3(a). After the C_S is charged up during select time, $V_{select1}$ and $V_{select2}$ signals change during frame time, turning T_1/T_2 OFF and T_4 ON, respectively. Then, the data current will flow from V_{dd} to ground through OLED, T_3, and T_4, which is indicated as a dotted line in Fig. 3(a). Same conditions for all the waveforms have been used except for the magnitude of V_{dd}, $V_{select1}$, and $V_{select2}$. The high and low values of $V_{select1}$ and $V_{select2}$ are 9 and 2 V, and 10 and 2 V, respectively.

$V_{select2}$ waveform was selected to produce 80% of duty ratio for light emission. V_{OLED} and V_{Cs} are voltage drop across the OLED and storage capacitor, respectively. I_{data}, I_{OLED}, and I_{GND} are current flow at data line, through OLED, and into GND, respectively, as indicated in Fig. 3(a). For the same I_{data} waveform, the storage capacitor is charged up to about 4.6 V during the select time and sustains the voltage during ON-time. OLED starts to be charged up to about 7.5 V at the beginning of the frame time and it sustains this value during ON-time. Similarly, the current peak during the selecting voltage transition was suppressed by optimizing $V_{select2}$ waveform. As simulated in Fig. 3(b), this pixel electrode circuit has duty ratio controllability of the OLED light emission by changing $V_{select2}$ waveform. Since only n-type TFTs are used in this pixel electrode circuit configuration, this circuit configuration can be easily applied to a-Si:H TFTs AM-OLED. It should be noted that the pixel electrode aperture ratio is much larger for top-anode OLED in comparison with the top-cathode OLED. In latter case, it is possible to define ITO electrode. It is not clear at this time which OLED structure, common cathode (GND) or common anode (Vdd), would be preferred for AM-OLEDs. Each pixel electrode structure has certain advantages and disadvantages, which will be discussed in the separate publication in the near future.

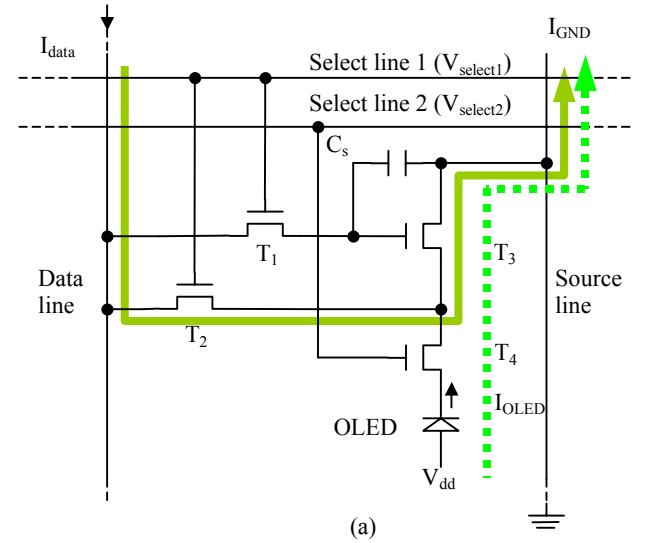

(a)

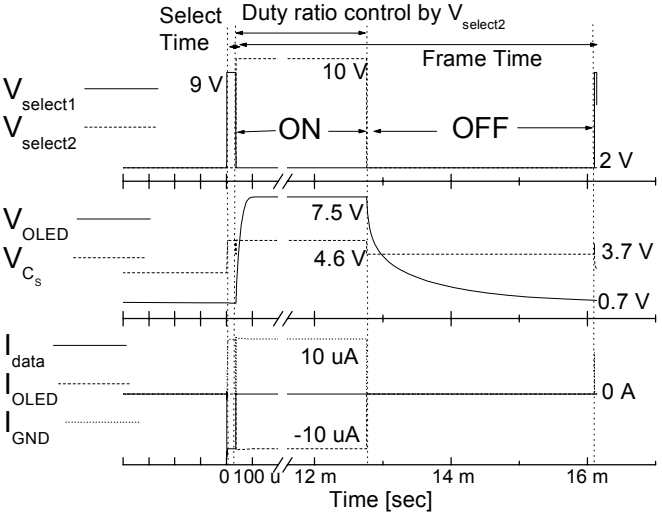

(b)

Figure 3. Four n-type poly-Si pixel electrode circuit for top-anode OLED structure and signal waveforms are shown. The bold arrow shows the current flow path charging storage capacitor during the select time. Since only n-type TFTs are considered, this type of pixel electrode circuit can also be applied to the a-Si:H TFT AM-OLED.

4. Conclusions

In this paper, we propose a current-sink type novel pixel electrode circuit consisting of four p-type or n-type poly-Si TFTs for top-cathode and top-anode OLED structures, respectively. The AIM-SPICE simulation shows that our new approach effectively decouples OLED from the data line by avoiding current flow through the OLED during the select time. It is also noted that our pixel electrode circuit provides the duty ratio controllability of light-emission needed for the high quality fast moving images.

5. Acknowledgements

This work was supported by NIH grant.

6. References

[1] Dawson, R.M.A., Shen, A., Furst, D.A., Connor, S., Hsu, J., Kane, M.G., Stewart, R.G., Ipri, A., King, C.N., Green, P.J., Flegal, R.T., Pearson, S., Barrow, W.A., Dickey, E., Ping, K., Robinson, S., Tang, C.W., Van Slyke, S., Chen, F., Shi, J., Lu, M.H.., and Sturm, J.C., *IEDM '98*, 875 (1998).

[2] Haskal, E.I., Buechel, M., Sempel, A., Heeks, S.K., Athanassopoulou, N., Carter, J.C., Wu, W., O'Brien, J. Fleuster, M., and Visser, R. J., *Proceedings of Asia Display '01*, 1411 (2001).

[3] Hattori, R., Kuroki, Y., and Kanicki, J., *AM-LCD '01*, 223 (2001).

[4] He, Y,. Hattori, R., and Kanicki, J., *IEEE Elec. Dev. Lett.* **21**, 590 (2000).

[5] He, Y., Hattori, R., and Kanicki, J., *IEEE Trans. Elec. Dev.* **48**, 1322 (2001).

[6] Hong, Y. and Kanicki, J., *Proceedings of Asia Display '01*, 1443 (2001).

[7] Jacunski, M.D., Shur, M.S., Owusu, A.A., Ytterdal, T., Hack, M., and Iniguez, B., *IEEE Trans. Elect. Dev.* **46**, 1146 (1999).

[8] Miyashita, S., Imamura, Y., Takeshita, H., Atobe, M., Yokoyama, O., Matsueda, Y., Miyazawa, T., Nishimaki, M., *Proceedings of Asia Display '01*, 1399 (2001).

[9] Sasaoka, T., Sekiya, M., Yumoto, A., Yamada, J., Hirano, T., Iwase, Y., Yamada, T., Ishibashi, T., Mori, T., Asano, M., Tamura, S., and Urabe, T., *Digest of SID '01*, 384 (2001).